Supporting Information

Development of Fluorometric Gamma Dosimeter Based on BODIPY-LMG Dye Loaded Superporous Polymer

Manoj K. Choudhary,[a,d] Sunita Gamre,[a] Narendra Kumar Goel,[b] Bhaskar Sanyal[c] and Soumyaditya Mula*[a,d]

[a]Bio-Organic Division, Bhabha Atomic Research Centre, Mumbai 400085, India.

[b]Radiation Technology Development Division, Bhabha Atomic Research Centre, Mumbai 400085, India.

[c]Food Technology Division, Bhabha Atomic Research Centre, Mumbai 400085, India.

[d]Homi Bhabha National Institute, Anushakti Nagar, Mumbai 400094, India.

E-mail: smula@barc.gov.in

Content

Materials and General Methods

All chemical reactions were conducted under an argon atmosphere utilizing anhydrous solvents in a screw-cap Schlenk tube. Reagents and solvents were sourced from a local supplier and used as received, without additional purification. Reaction progress was monitored *via* thin-layer chromatography on commercially available 0.25 mm fluorescent silica plates (F-254), visualized under a UV lamp at 254 nm and 354 nm wavelengths. Purification of compounds was performed by column chromatography using silica gel (250–400 mesh). NMR spectra were obtained on a 500 MHz Varian FT-NMR instrument. High Resolution Mass Spectrometric (HRMS) analysis was performed using 6540 UHD Accurate-Mass Agilent Q-TOF LC/MS instrument, WATERS Micromass Q-TOF MicroTM instrument and Bruker Maxis Impact Micro-TOF LC/MS instrument. SEM was recorded using ZEISS-EVO 25 instrument.

JASCO make UV–vis spectrophotometer (Model: V 670) was used for recording steady state absorption spectra with samples taken in a quartz cuvette of 1 cm path length. Steady-state emission studies were performed using a JASCO make spectrofluorometer (Model: FP 6500) with samples in a 10 mm × 10 mm optical cell.

Photography for the solid state dosimetry was done using NIKON D5600 DSLR camera (24 megapixels, CMOS sensor, ISO-A (100-25600), shutter speed range: 1/4000 sec- 30 sec, F-Stop: f/5 – f/32, Lens: Nikon AF-S DX Nikkor 18-140 mm f/3.5-5.6G ED VR Lens). Photography under UV light was done using the specifications: F-stop: f/16, exposure time: 1/50 sec, ISO-A: 25600, focal length: 140 mm, maximum aperture: 4.7, exposure mode: manual. On the other hand, photography under visible light was done using the specifications: F-stop: f/5.6, exposure time: 1/80 sec, ISO-A: 800, focal length: 42 mm, maximum aperture: 4.3, exposure mode: manual.

Superporous poly(2-hydroxyethyl methacrylate) (PolyHEMA) and PGMA-g-PolyHEMA were investigated to assess morphological changes induced by radiation-assisted grafting. Scanning electron microscopy (SEM) was employed to visualize the surface and internal porous structure of the polymers. As the samples are inherently non-conductive, they were coated with a thin layer of gold via sputter coating to prevent charging and enhance image resolution. The coated samples were then mounted on SEM stubs using graphite tape to provide a conductive path and further avoid charge accumulation during imaging.

Synthesis and NMR spectra

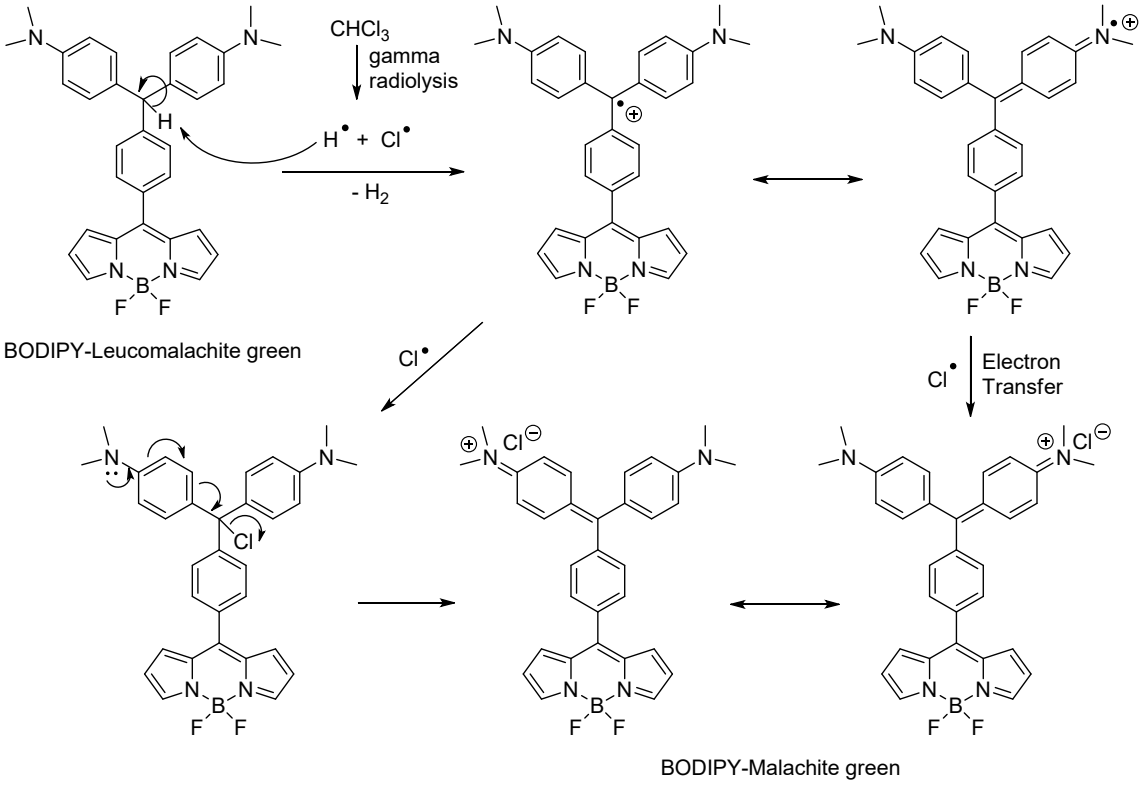

Scheme S1. Mechanism for conversion of BODIPY-Leucomalachite green dye (**3**) to BODIPY-Malachite green dye (**4**) under gamma radiolysis in chloroform.

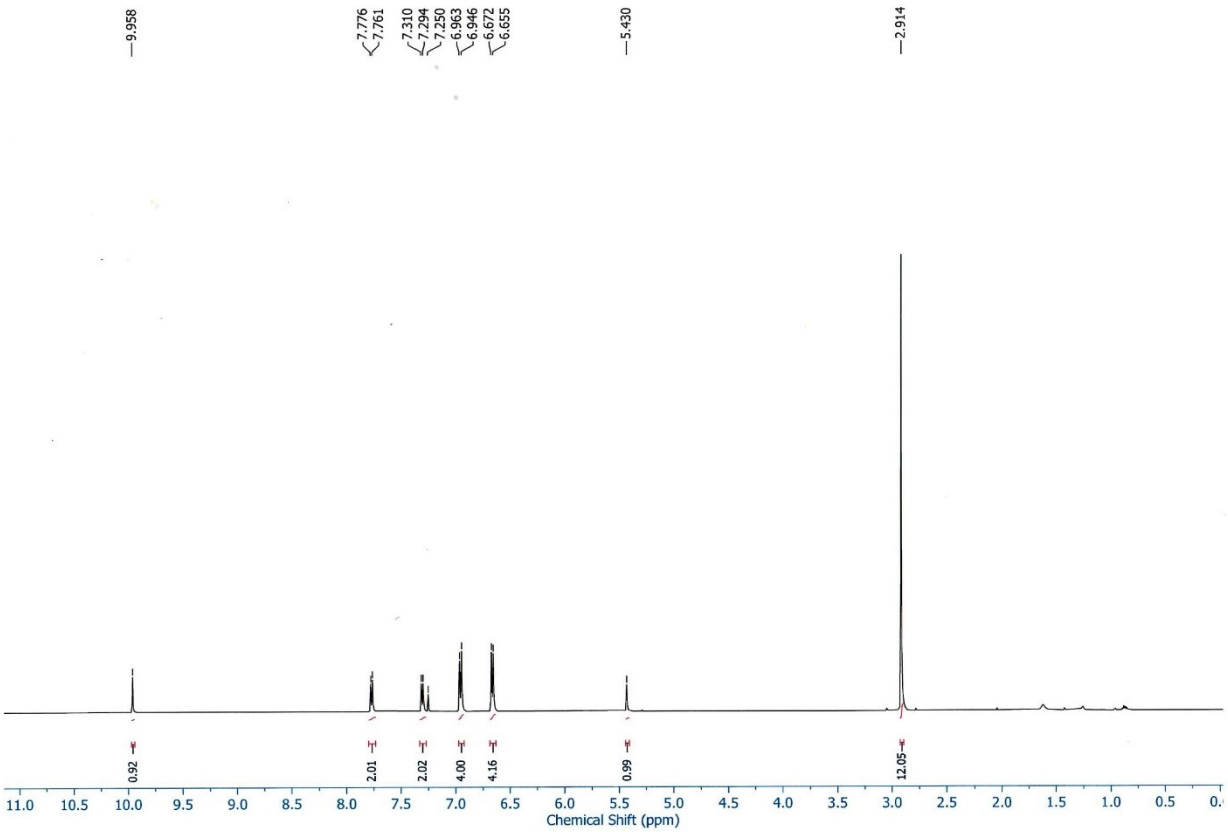

Figure S1. ^{1}H NMR of **7** in $CDCl_3$.

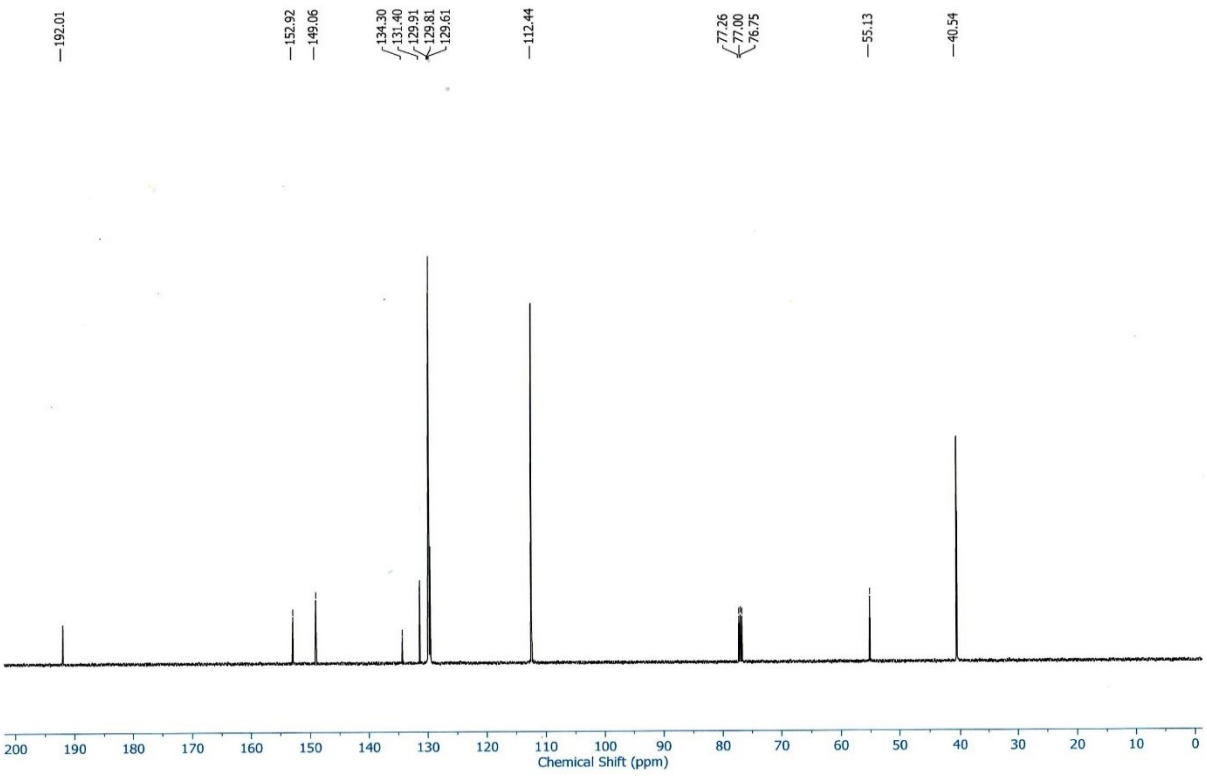

Figure S2. ^{13}C NMR of **7** in $CDCl_3$.

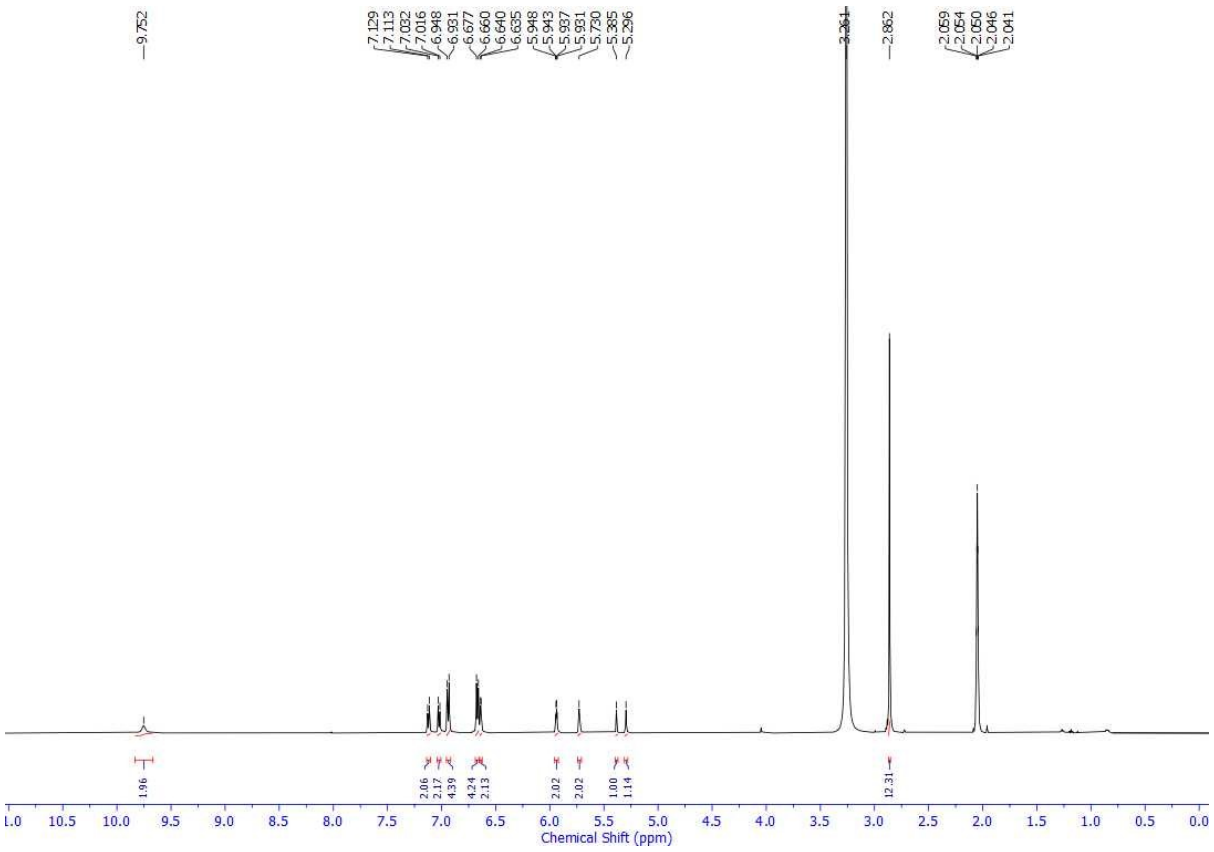

Figure S3. ^{1}H NMR of **8** in in Acetone-d_6.

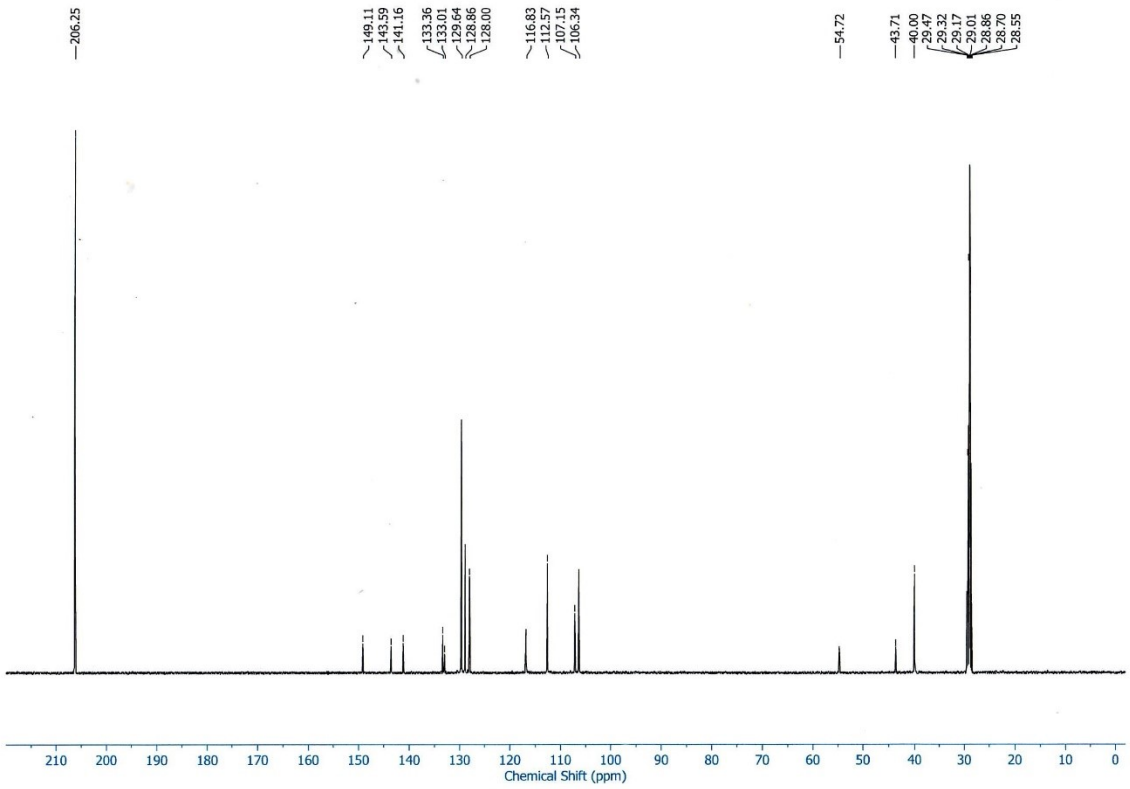

Figure S4. ^{13}C NMR of **8** in in Acetone-d_6.

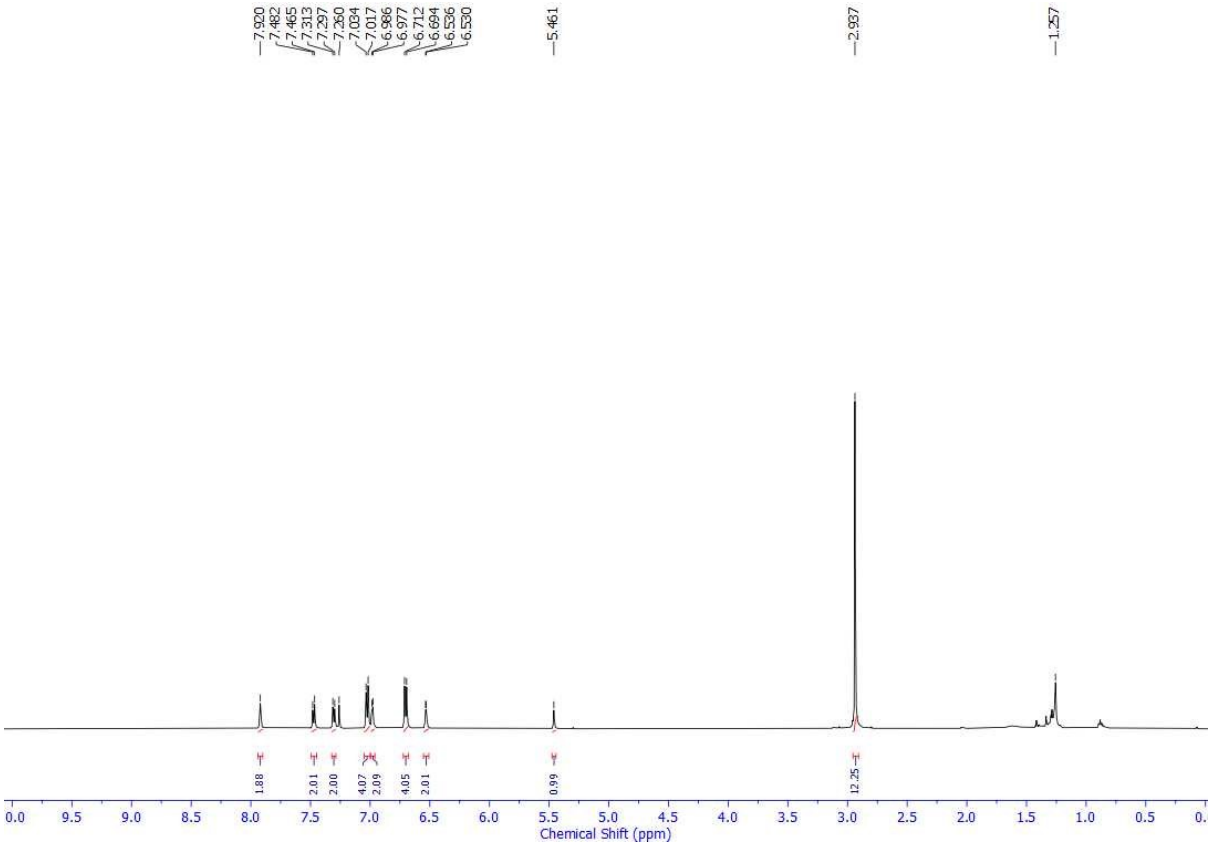

Figure S5. ^{1}H NMR of BLMG **3** in $CDCl_3$.

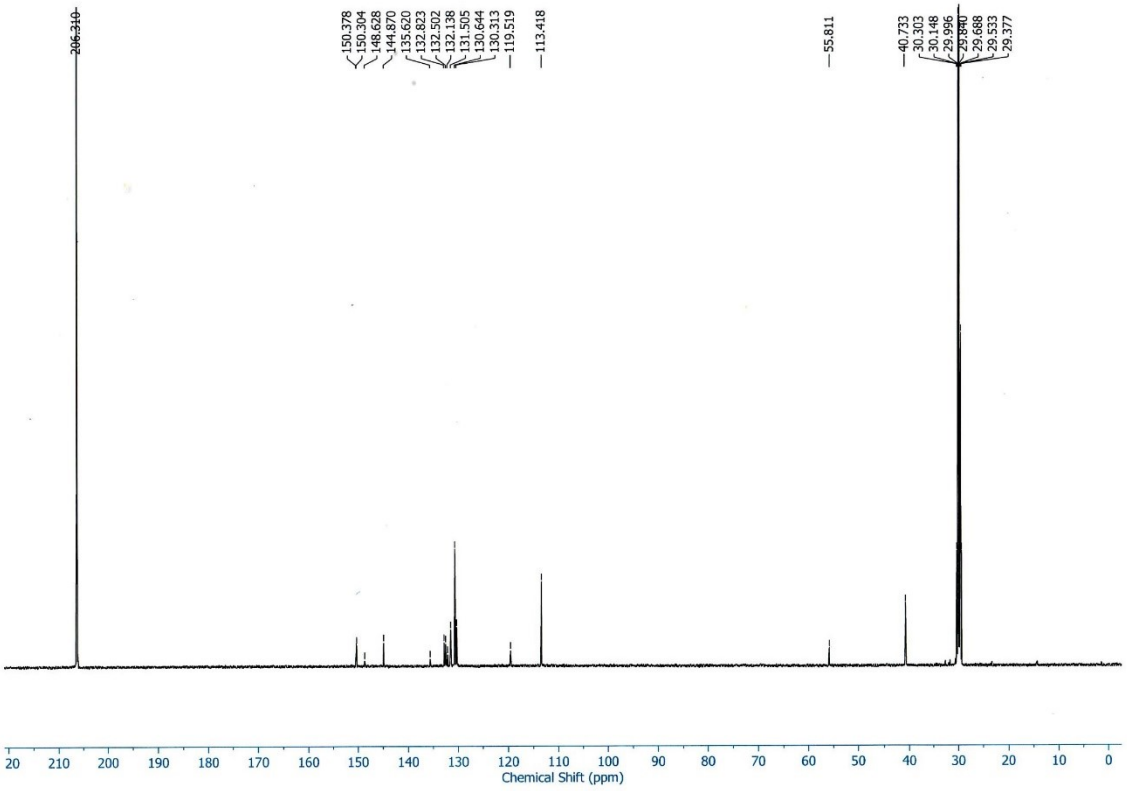

Figure S6. ^{13}C NMR of BLMG **3** in Acetone-d_6.

Synthesis of PolyGMA grafted PolyHEMA

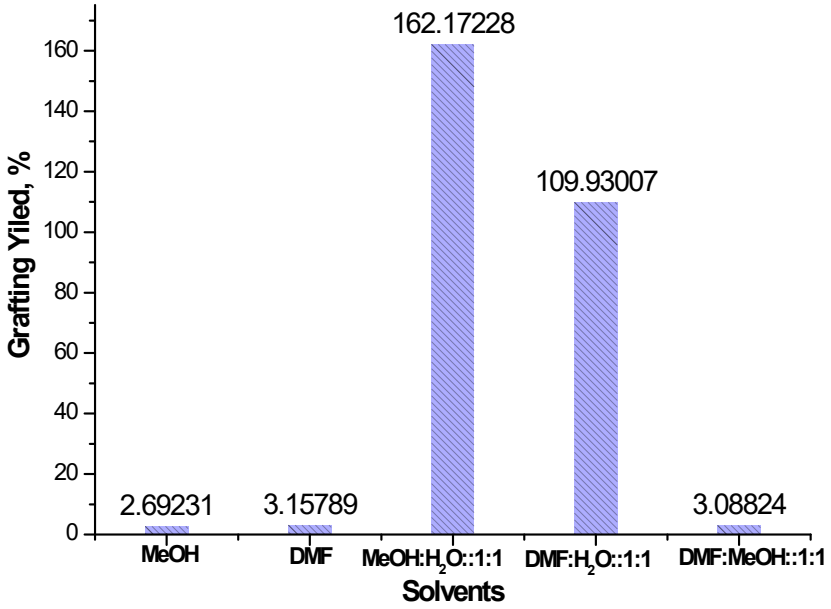

Figure S7. Effect of solvents on to grafting extent of GMA on to SPH @ 12.5% GMA.

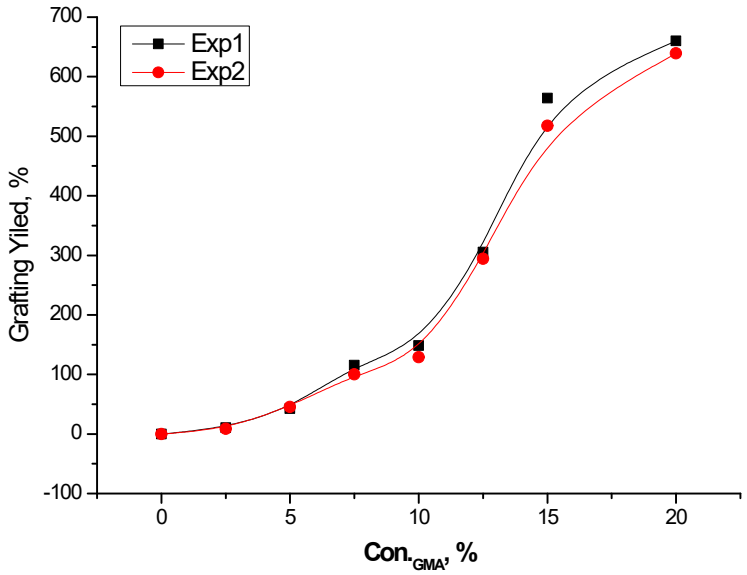

Figure S8. Effect of GMA concentration on to grafting extent on to superporuos polyHEMA at total absorbed dose of 5k Gy in MeOH/H_2O (1:1).

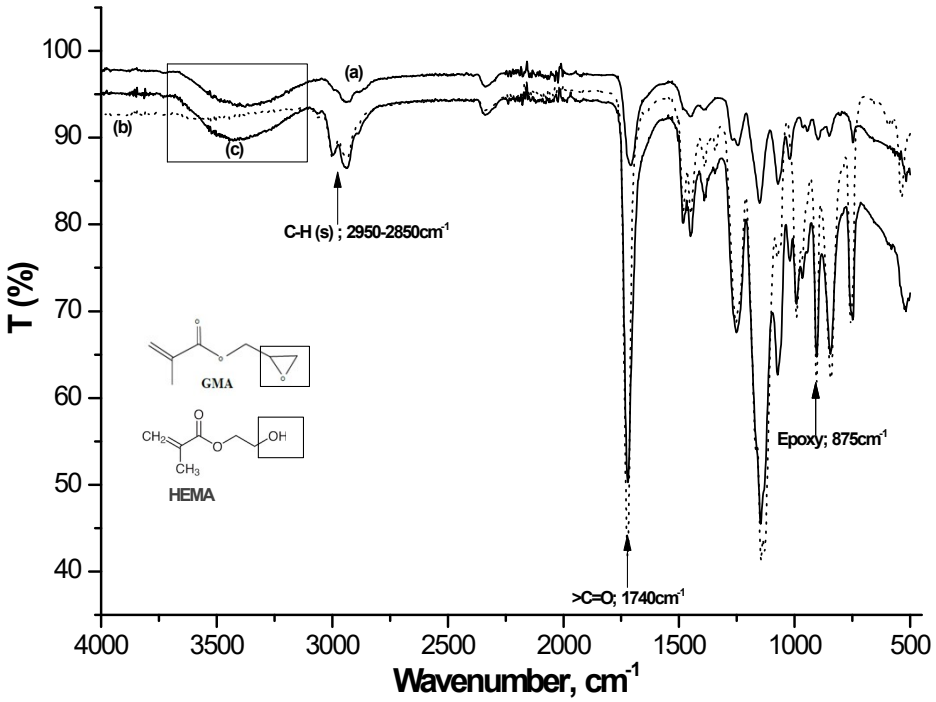

Figure S9. FTIR spectra of (a) untreated poly(HEMA) and (b) Poly(GMA) (c) PolyGMA-g-poly(HEMA) (G.Y.~100%).

Photophysical property studies

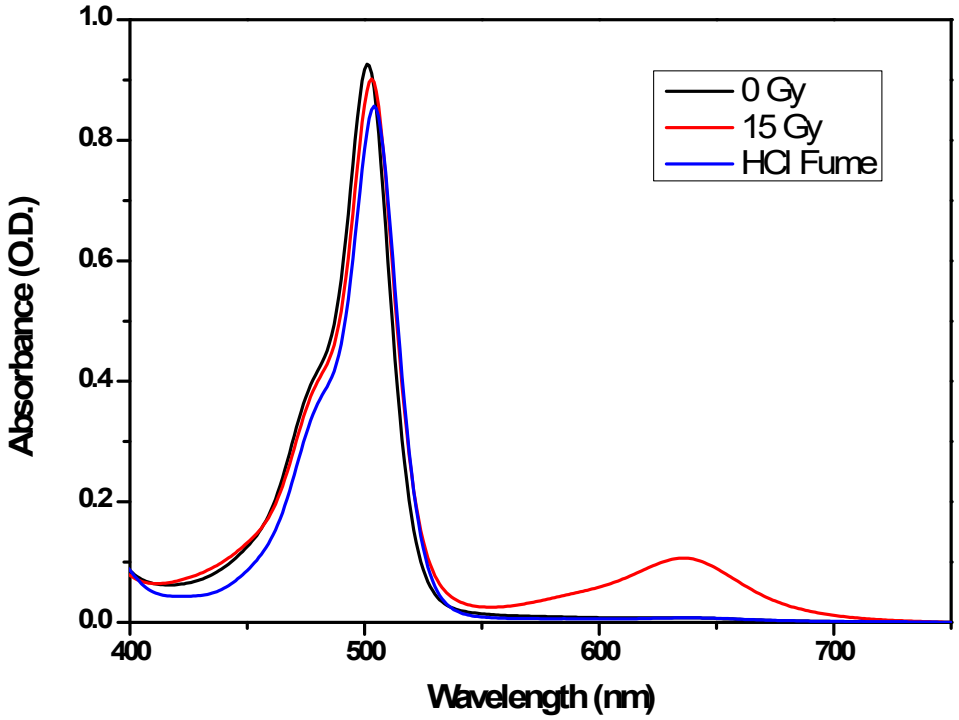

Figure S10. Change in absorption spectra of BLMG **3** with HCl exposure and after 15 Gy of γ–radiation exposure in chloroform.

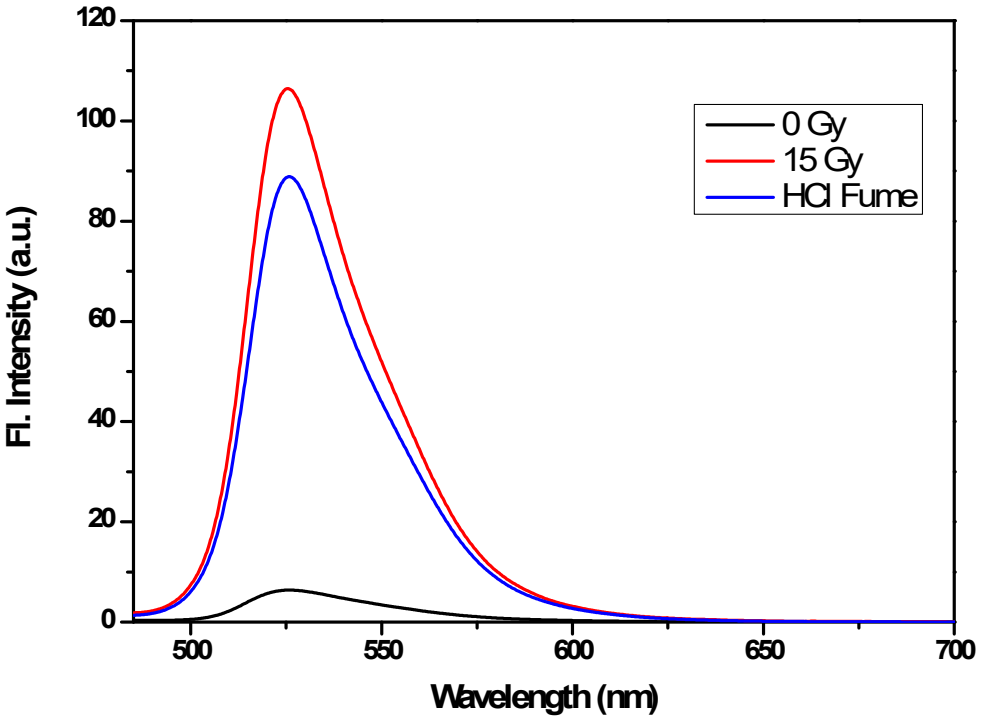

Figure S11. Change in fluorescence spectra of BLMG **3** with HCl exposure and after 15 Gy of γ–radiation exposure in chloroform.

Gamma dosimetry studies

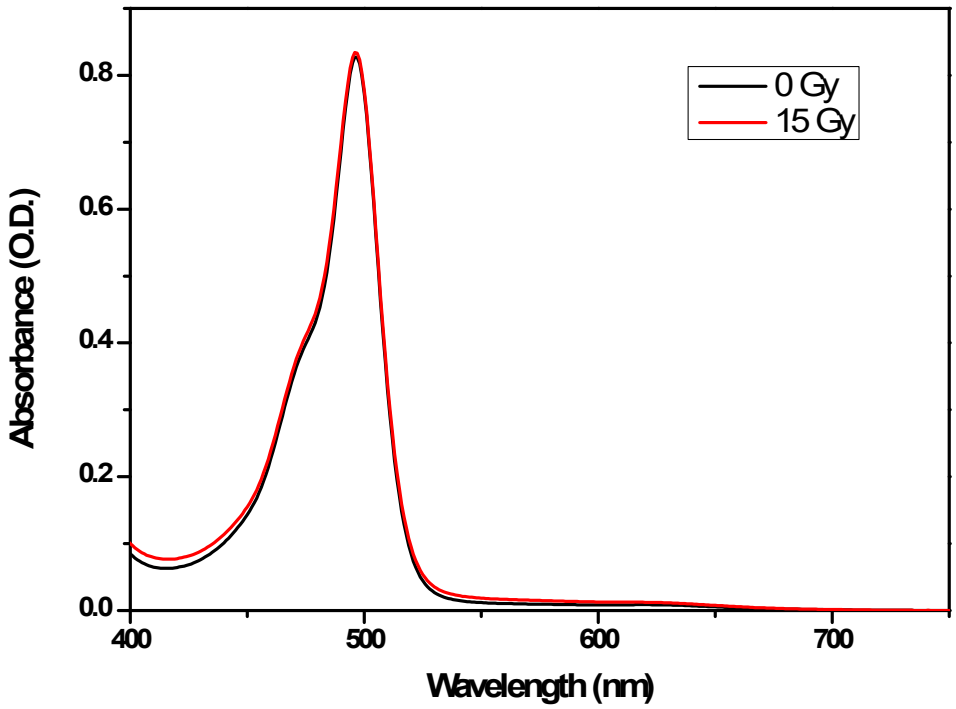

Figure S12. Absorption spectra of BLMG **3** in ACN before and after γ-irradiation (15 Gy).

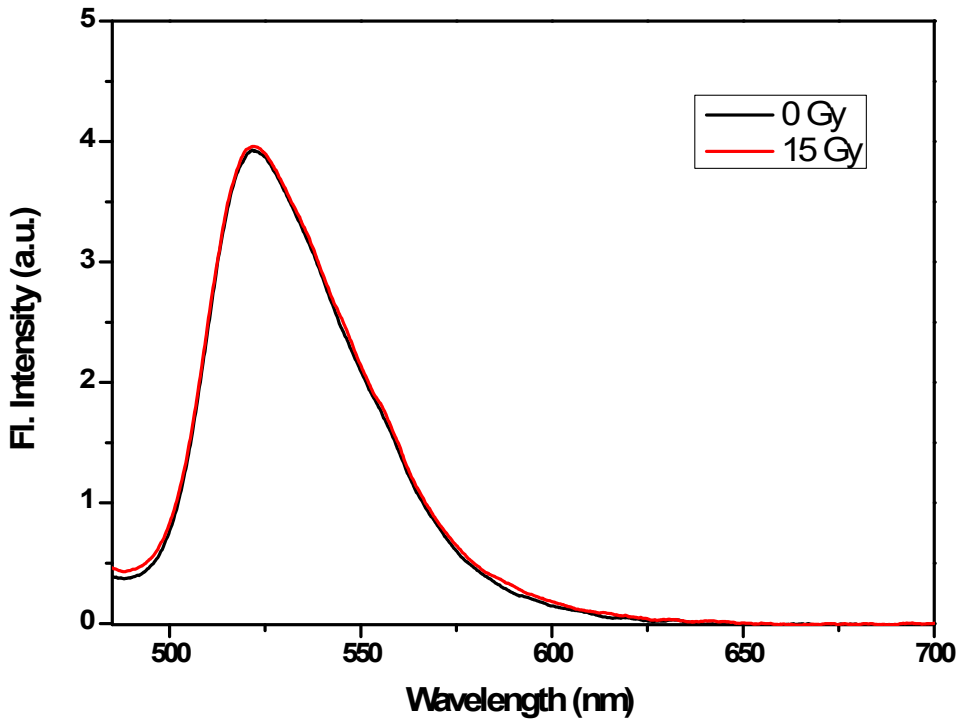

Figure S13. Fluorescence spectra of BLMG **3** in ACN before and after γ-irradiation (15 Gy).

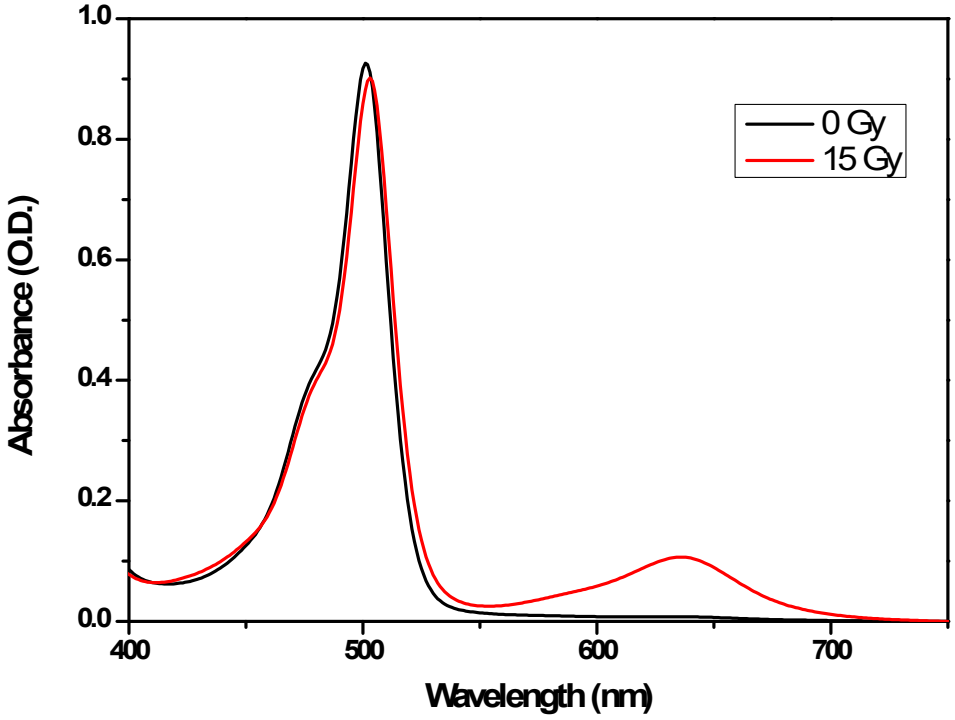

Figure S14. Absorption spectra of BLMG **3** in $CHCl_3$ before and after γ-irradiation (15 Gy).

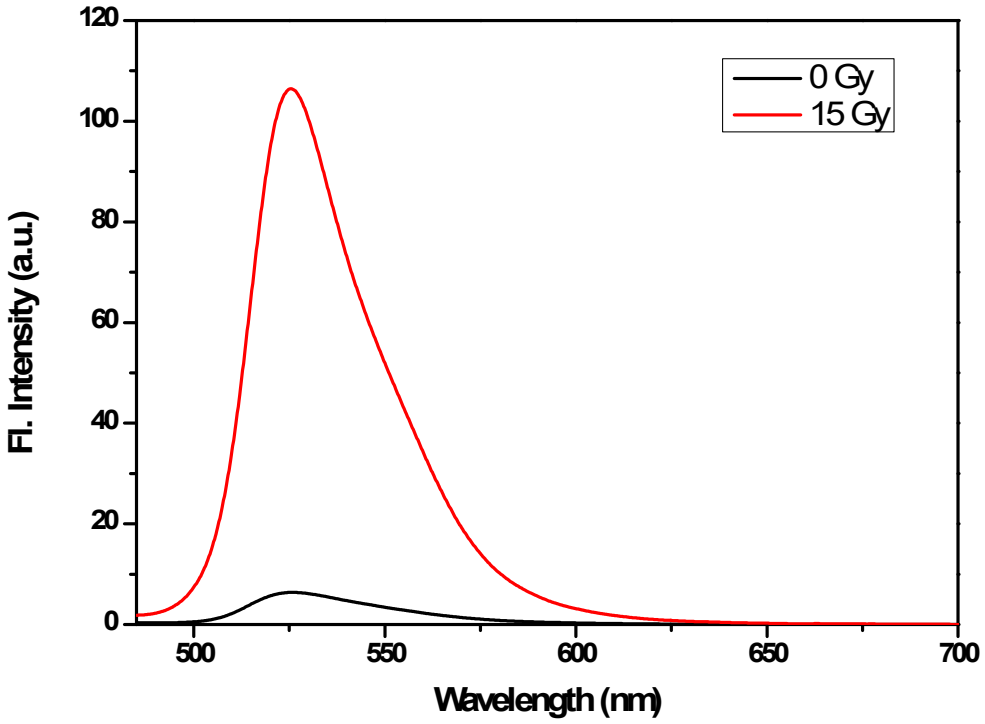

Figure S15. Fluorescence spectra of BLMG **3** in $CHCl_3$ before and after γ-irradiation (15 Gy).

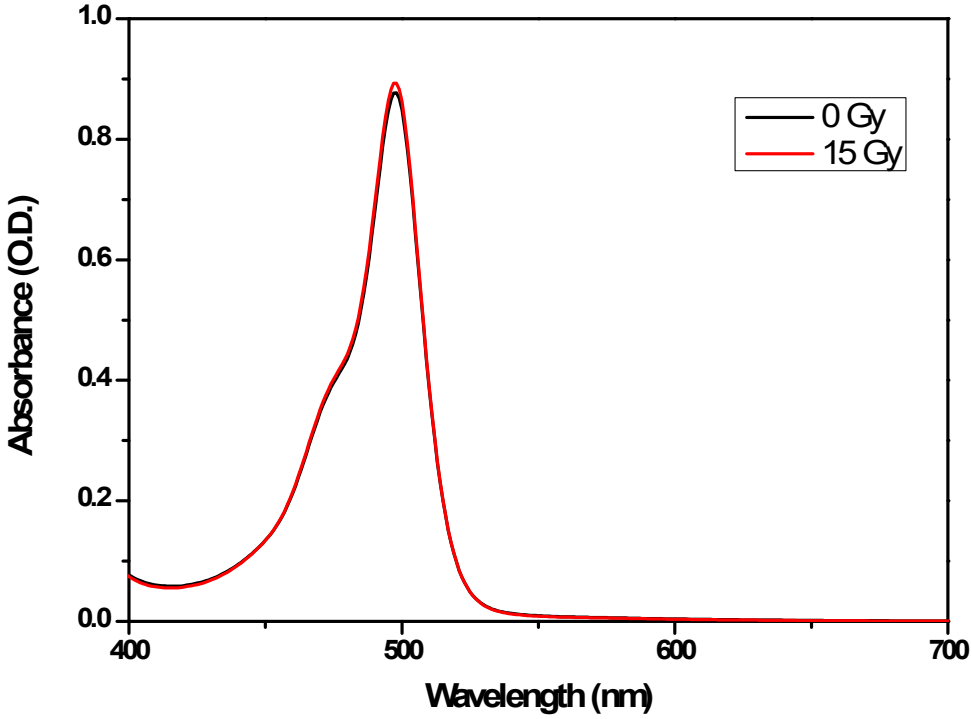

Figure S16. Absorption spectra of BLMG **3** in EtOAc before and after γ-irradiation (15 Gy).

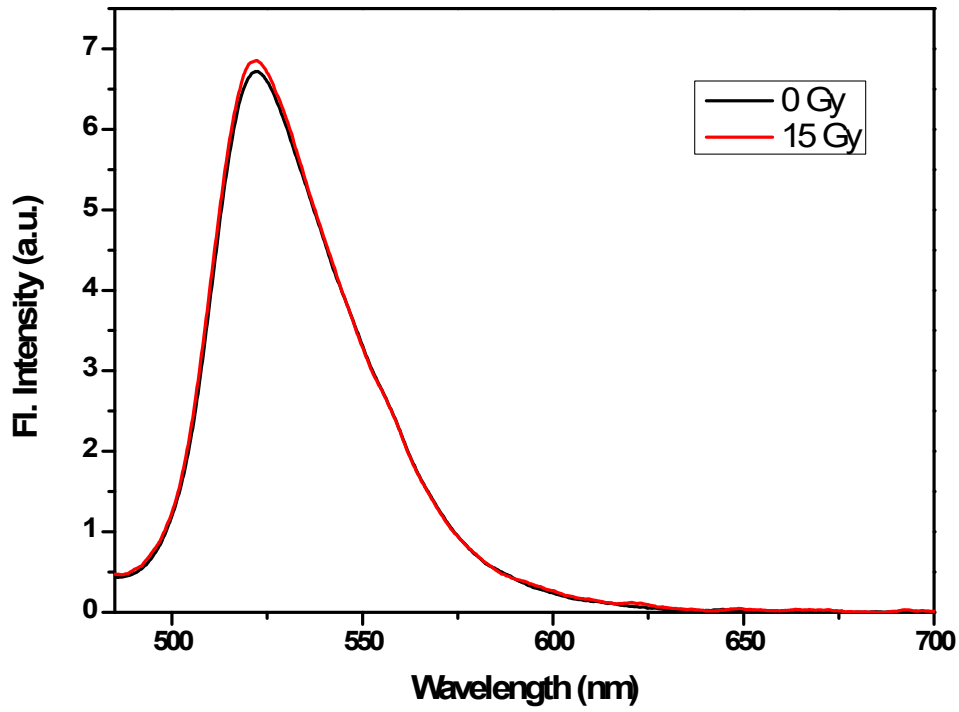

Figure S17. Fluorescence spectra of BLMG **3** in EtOAc before and after γ-irradiation (15 Gy).

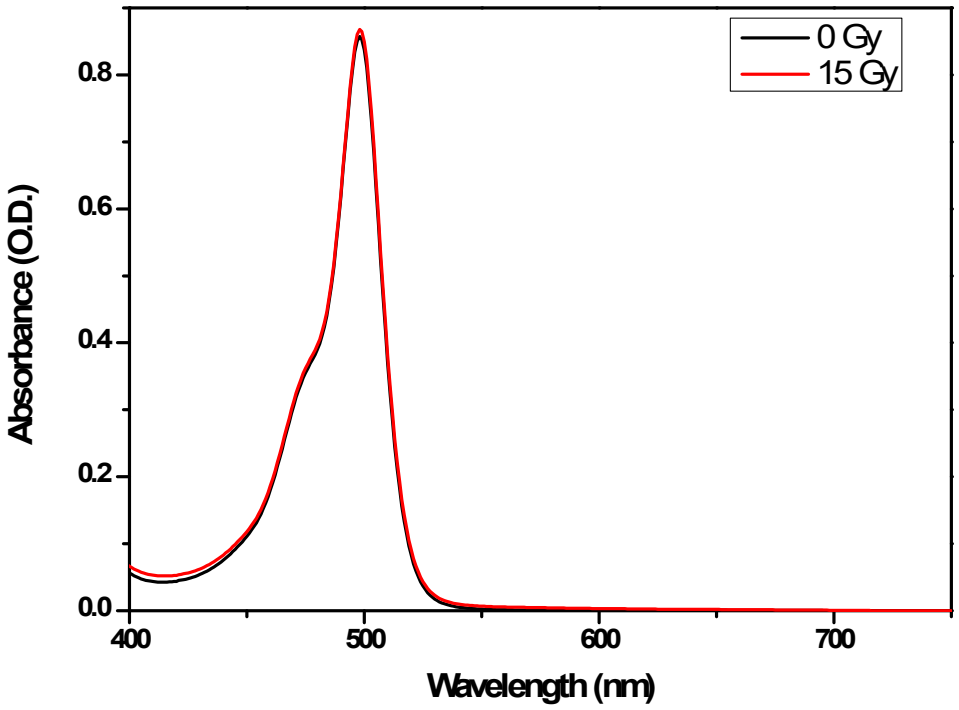

Figure S18. Absorption spectra of BLMG **3** in hexane before and after γ-irradiation (15 Gy).

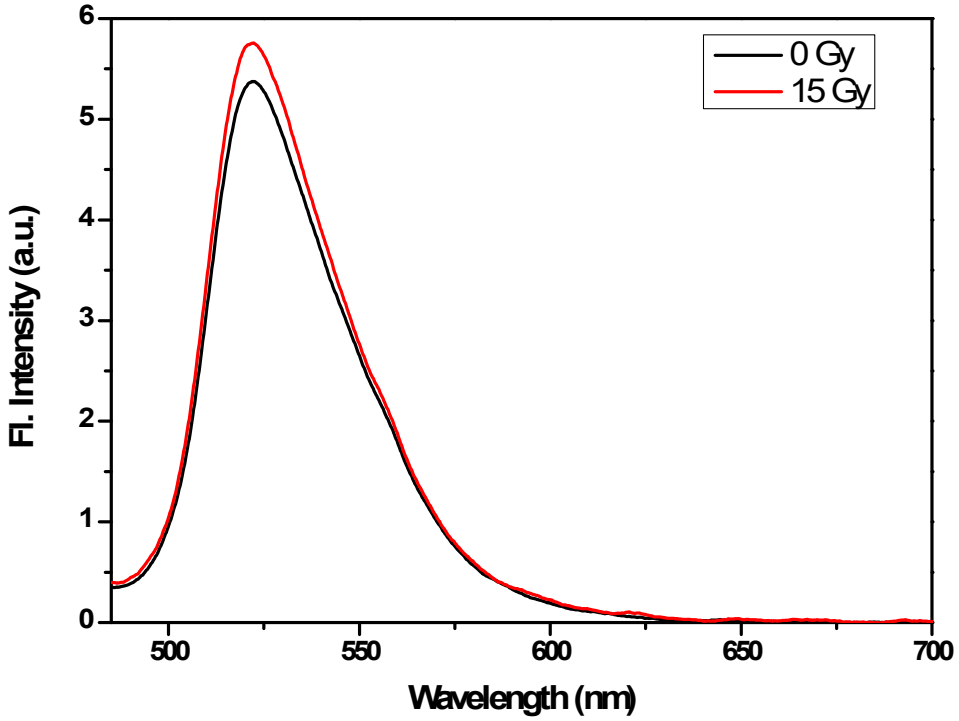

Figure S19. Fluorescence spectra of BLMG **3** in hexane before and after γ-irradiation (15 Gy).

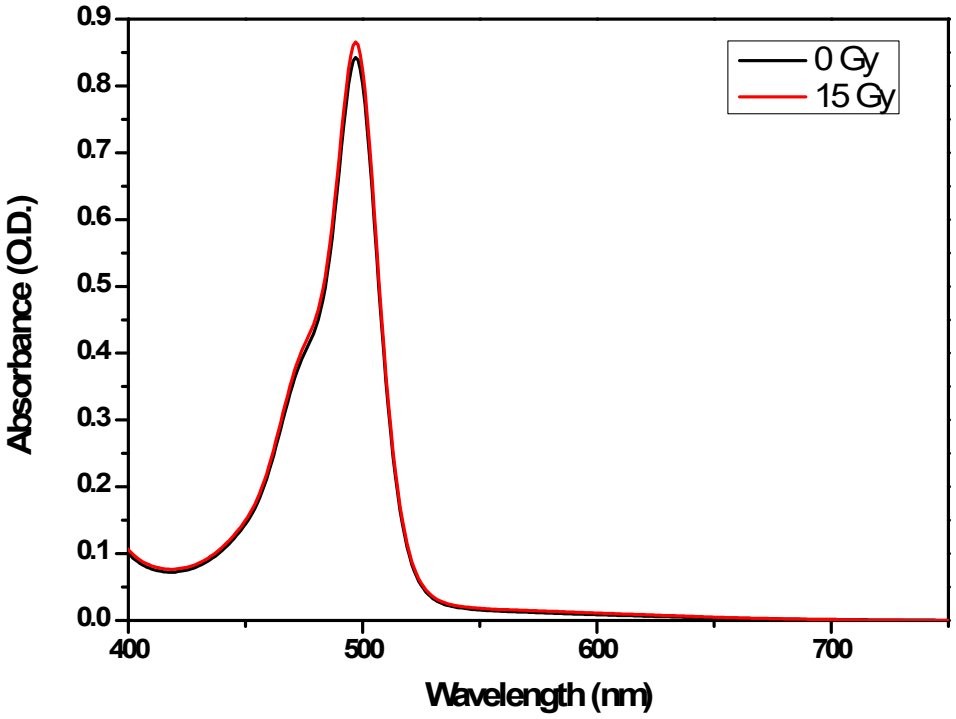

Figure S20. Absorption spectra of BLMG **3** in MeOH before and after γ-irradiation (15 Gy).

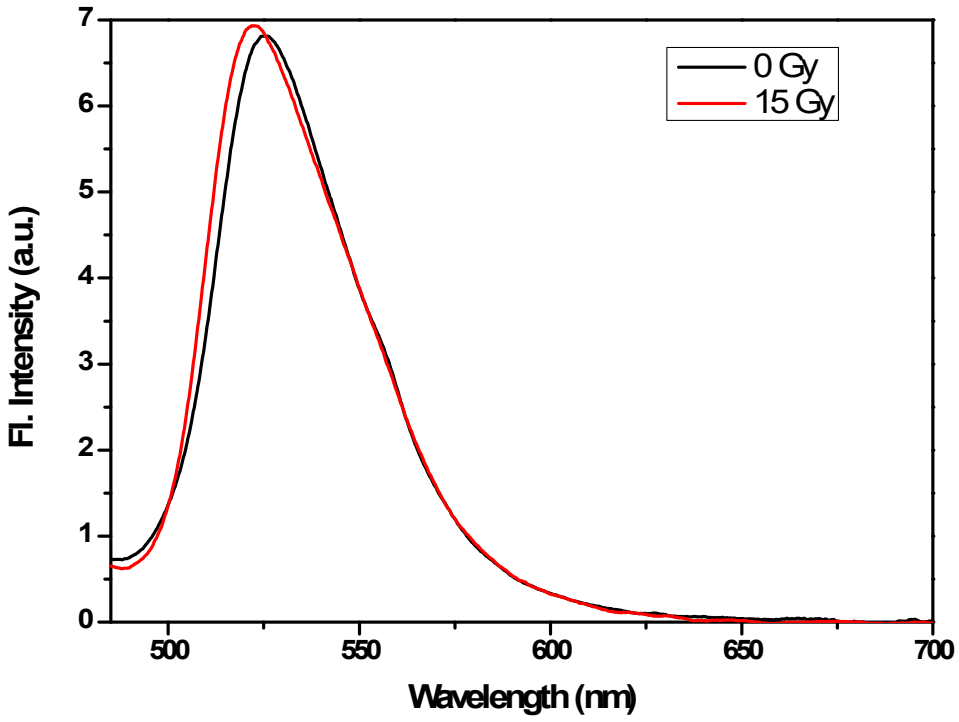

Figure S21. Fluorescence spectra of BLMG **3** in MeOH before and after γ-irradiation (15 Gy).

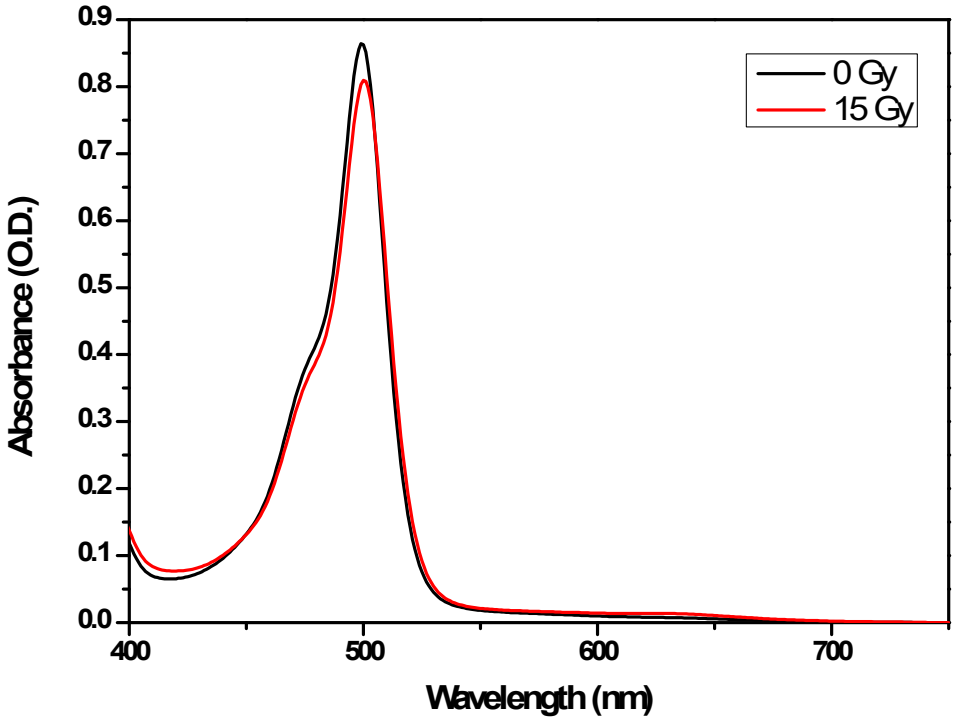

Figure S22. Absorption spectra of BLMG **3** in THF before and after γ-irradiation (15 Gy).

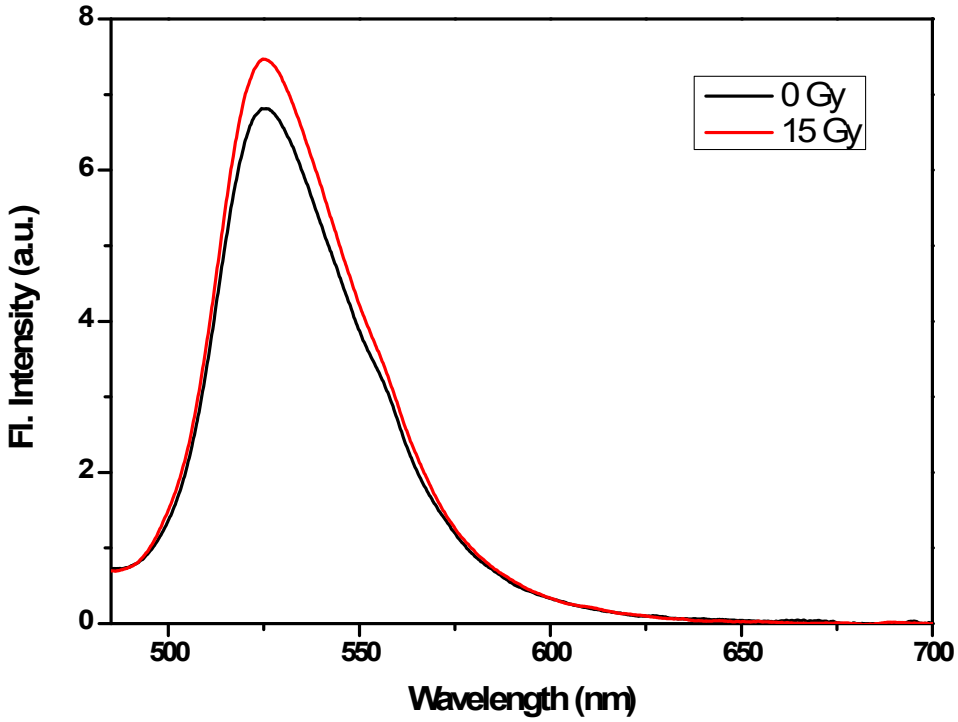

Figure S23. Fluorescence spectra of BLMG **3** in THF before and after γ-irradiation (15 Gy).

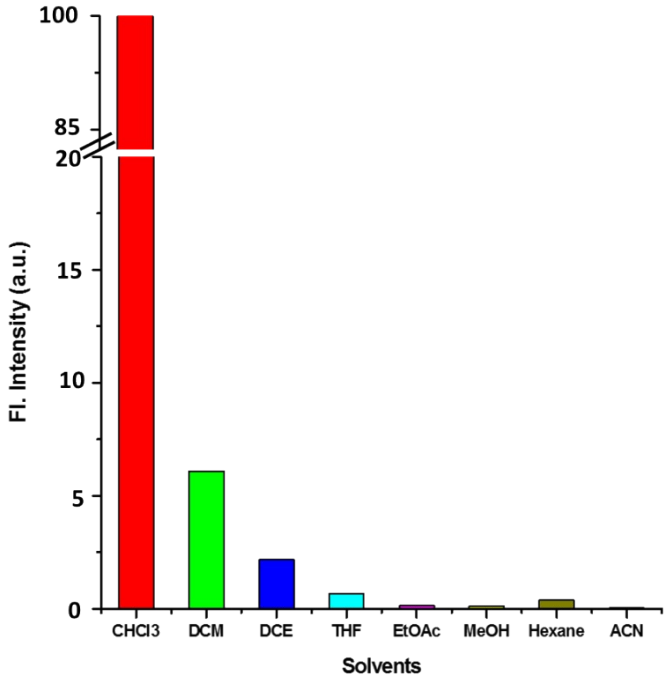

Figure S24. Fluorescence intensity of BLMG **3** in different solutions after 15 Gy of γ-irradiation.

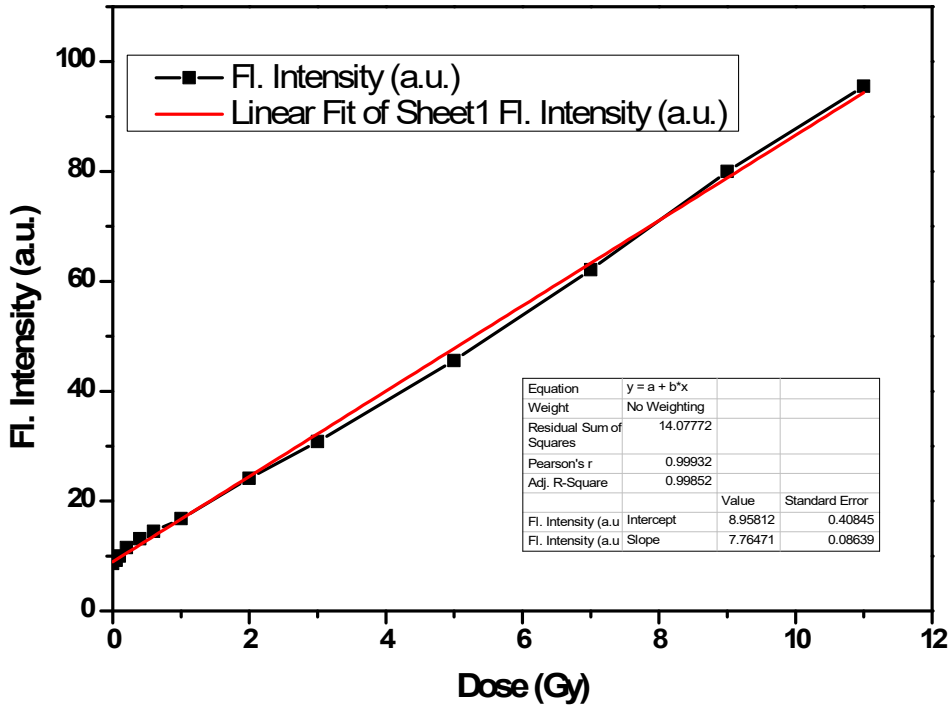

Figure S25. Linear Fit of plot of fluorescence enhancement of BLMG **3** (20 μM) with γ-radiation dose.

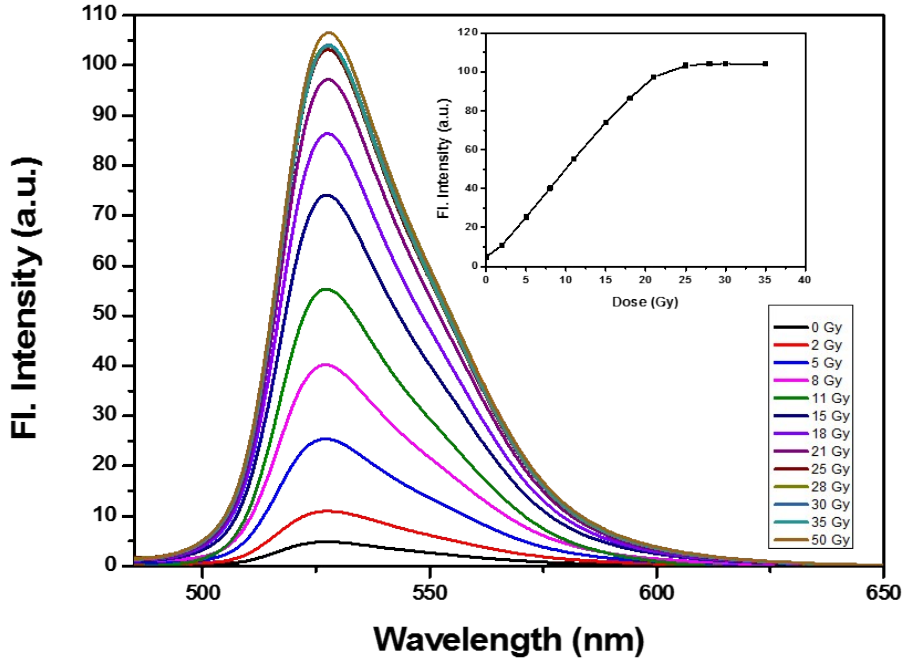

Figure S26. Fluorescence profile change of BLMG **3** (40 μM, λ_{ex} = 485 nm) in $CHCl_3$ under increasing γ-radiation exposure (0-50 Gy). Inset: Plot of fluorescence enhancement of BLMG **3** with γ-radiation dose.

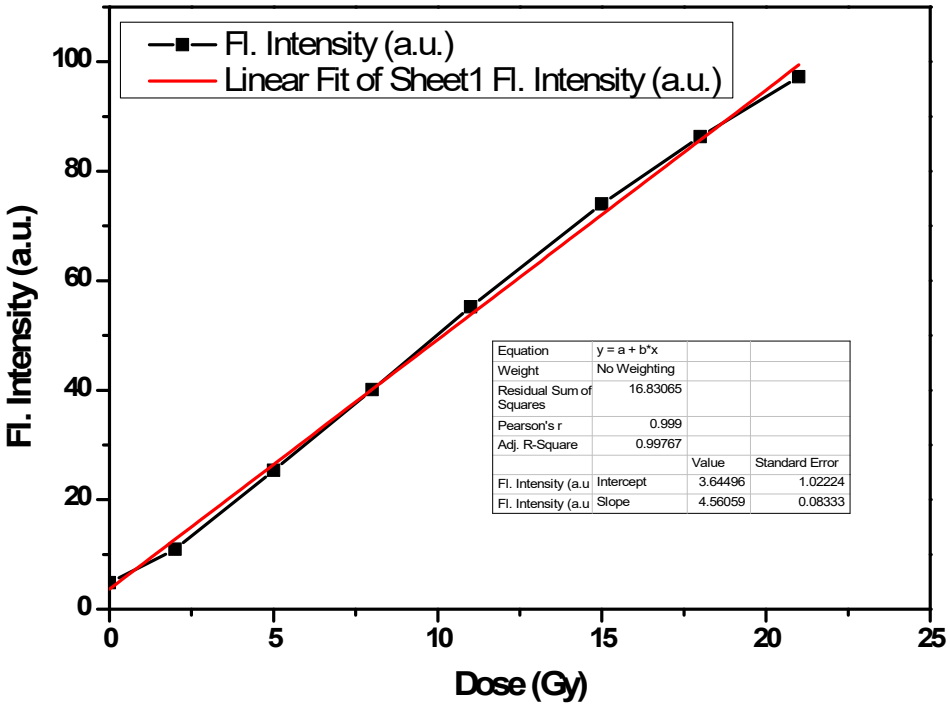

Figure S27. Linear Fit of plot of fluorescence enhancement of BLMG **3** (40 μM) with γ-radiation dose.

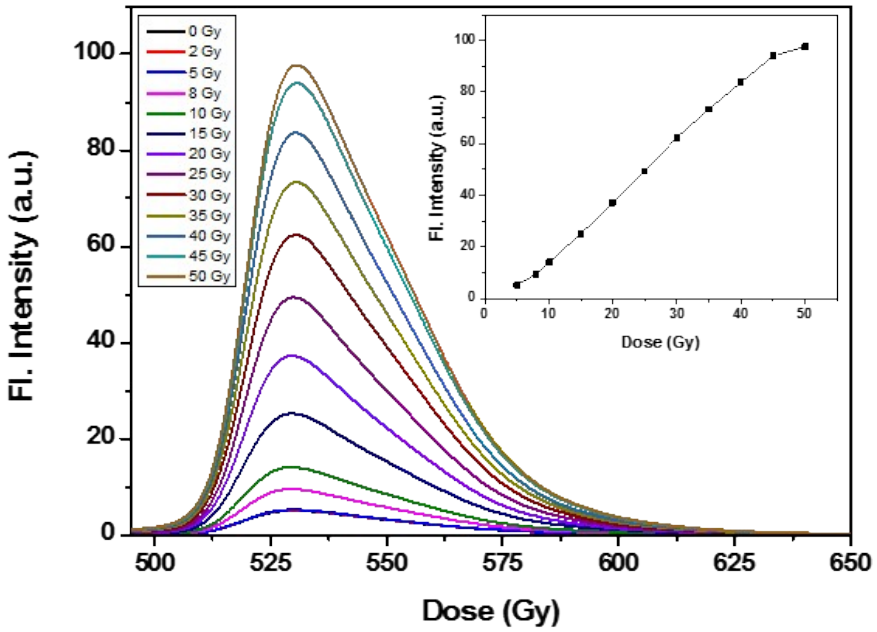

Figure S28. Fluorescence profile change of BLMG **3** (80 μM, λ_{ex} = 485 nm) in $CHCl_3$ under increasing γ-radiation exposure (0-50 Gy). Inset: Plot of fluorescence enhancement of BLMG **3** with γ-radiation dose.

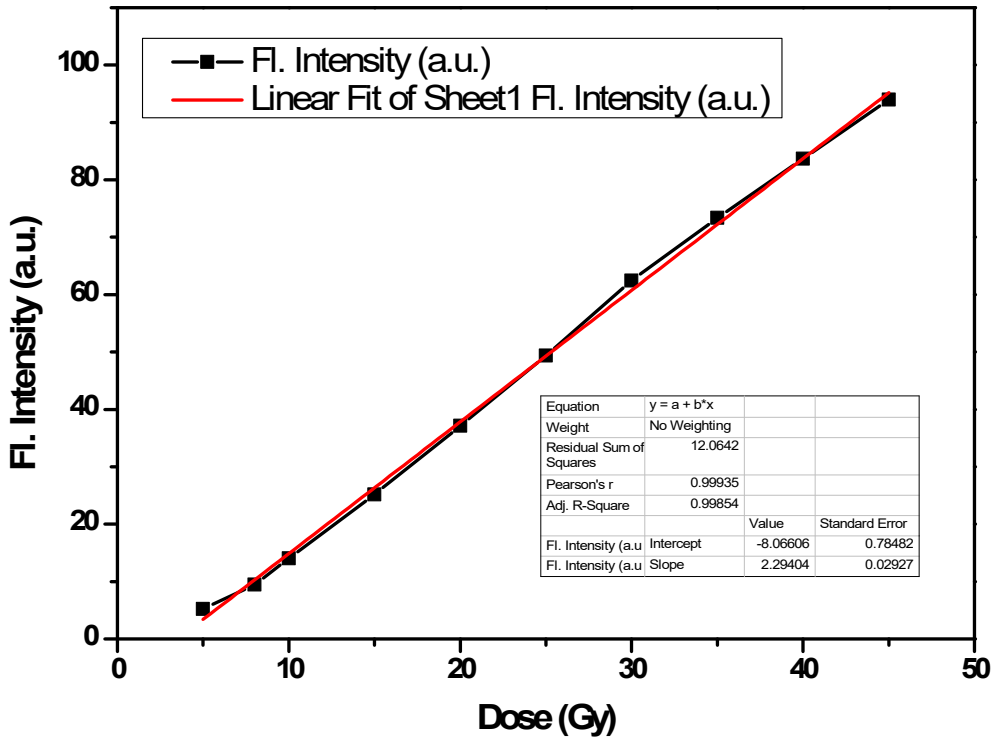

Figure S29. Linear Fit of plot of fluorescence enhancement of BLMG **3** (80 μM) with γ-radiation dose.

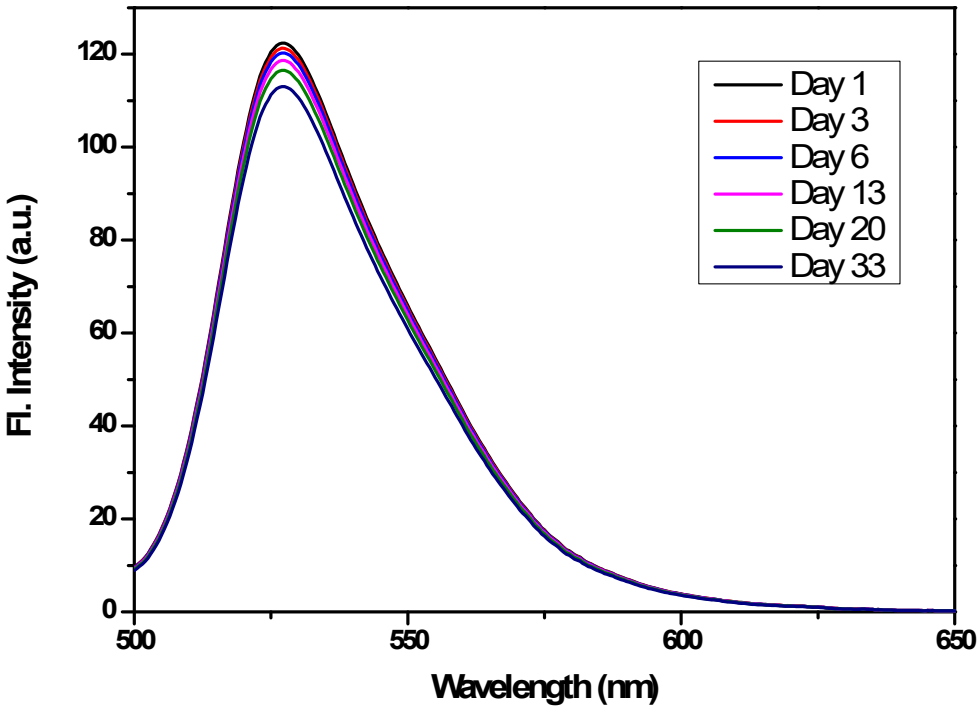

Figure S30. Stability of the fluorescence output of BLMG **3** in chloroform solution after gamma irradiation.

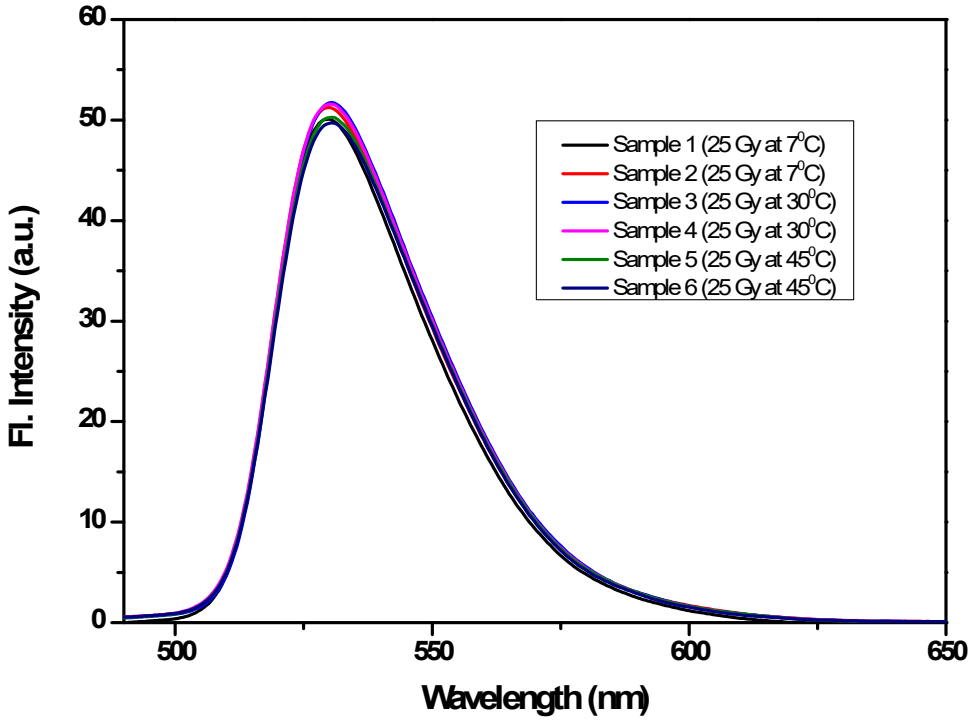

Figure S31. Fluorescence output of dosimeter with BLMG **3** in chloroform solution (80 μM) after 25 Gy of gamma irradiation (Dose rate: 54.40 Gy/min) under different temperature condition.

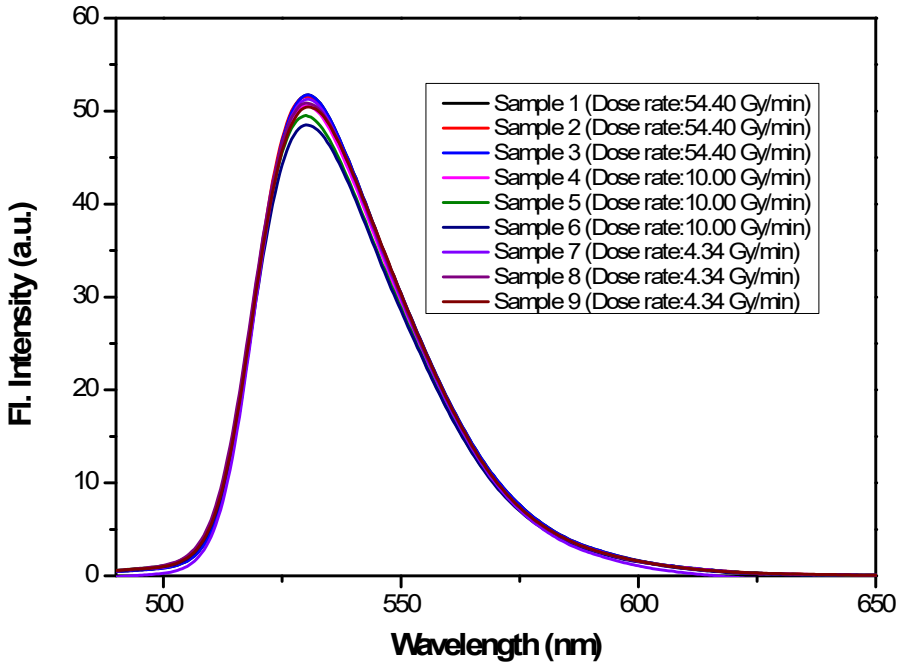

Figure S32. Fluorescence output of dosimeter with BLMG **3** in chloroform solution (80 μM) after 25 Gy of gamma irradiation with different dose rate.

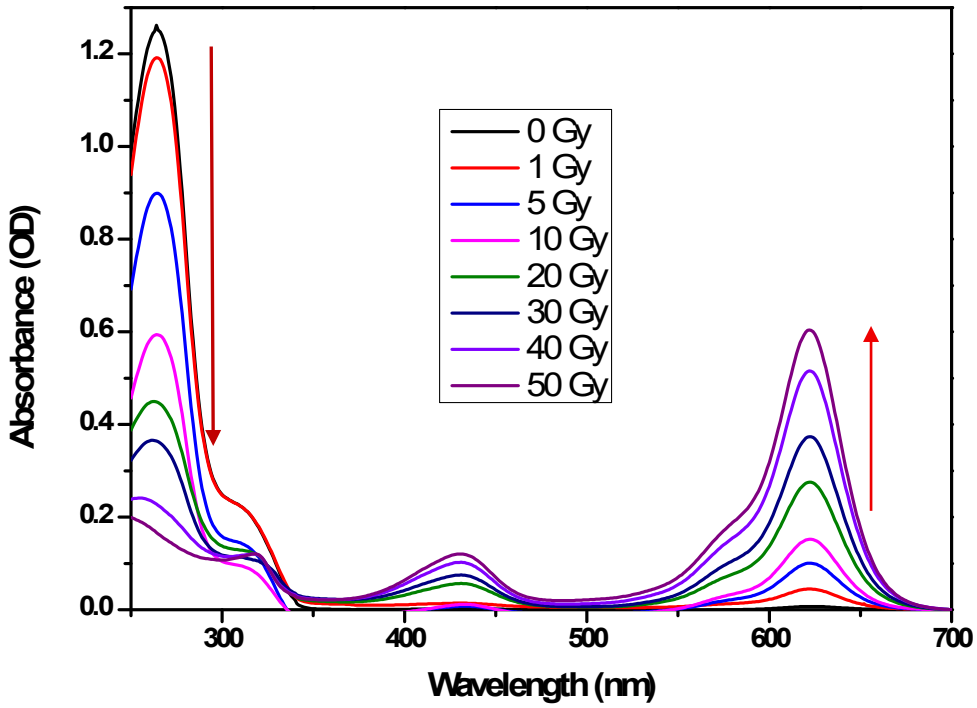

Figure S33. Absorbance profile change of LMG **1** (80 μM) in $CHCl_3$ under increasing γ-radiation exposure (0-50 Gy).

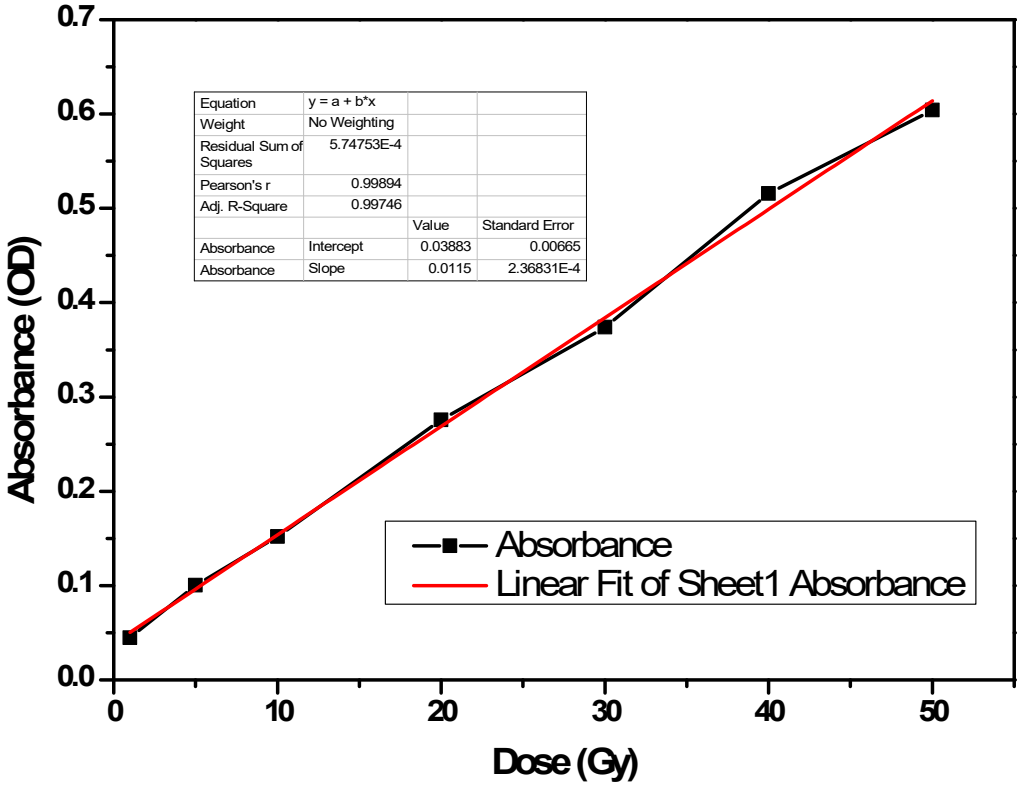

Figure S34. Linear Fit of plot of increase in absorbance of LMG **1** (80 μM) with γ-radiation dose.

Calculation of LOD: The Limit of Detection (LOD) was determined following the IUPAC protocol with the formula LOD = 3σ/S, where S represents the slope of the calibration curve, and σ is the standard deviation of the fluorescence response of the blank, obtained from 10 consecutive fluorescence measurements of the dye under consistent conditions.

LOD = (3 x 0.01657) / 7.7647

= 0.0064 Gy

Cost calculations: Fluorescence technique is known to be low-cost analytical technique. It requires fluorometer which is easily available with reasonable price. And the fluorophore is also required in very less quantity (mM to nM concentration). The synthetic cost of the BLMG dye (only chemicals cost) is Indian Rs. 3800/100 mg (~40 USD/100 mg). As we use 80 mM dye solution for 0-50 Gy measurement, thus from 10 mg BLMG dye we can make ~60 dosimeters. Thus, cost of each dosimeter will be very low (Indian Rs. 6 for each dosimeter). For lower dose range measurement, more diluted dye solution is required, in that case, the cost of each dosimeter will be further less.

Determination of Swelling Ratio:

To determine the Swelling Ratio, both grafted and non-grafted polymers were soaked in $CHCl_3$ for 10 min.

Sr. No	Wt. of polyHEMA (g)	Wt. of absorbed $CHCl_3$ (g)	Wt. of absorbed $CHCl_3$ per gram of polyHEMA	Swelling Ratio (Mean)
1	0.202□□	0.528	2.61	2.62
2	0.111	0.288□	2.59	
3	0.118	0.314□	2.66	

Table S1. Calculation of Swelling Ratio of superporous PolyHEMA (SPH).

Table S2. Calculation of Swelling Ratio of PolyGMA-g-PolyHEMA.

Sr. No	Wt. of polyHEMA in grafted polymer (g)	Wt. of absorbed $CHCl_3$ (g)	Wt. of absorbed $CHCl_3$ per gram of polyHEMA	Swelling Ratio (Mean)
1	0.794	12.47	15.71	15.86
2	0.519	8.62	16.61	
3	0.576	8.79□	15.26	

Ratio of "Swelling Ratio" of grafted polymer and non-grafted polymer = 15.86 / 2.62□ = 6.05

Table S3. Comparison of the developed γ–dosimeter with reference standard dosimetry systems.

Dosimeter	**Measurement instrument**	**Usable dose range (Gy)**	**Ref**
BLMG (20 μM)[a]	Fluorometer	0.006-11	Our Method
Calorimeter	Thermometer	10^2–10^5	1
Alanine	EPR spectrometer	1–10^5	1
Ceric-cerous sulphate	UV spectrophotometer or electrochemical potentiometer	5×10^2–5×10^4	1
ECB solution	Spectrophotometer, colour titration, high frequency conductivity	10–2×10^6	1
Ferrous sulphate solution	UV spectrophotometer	20–4×10^2	1
Dichromate solution	UV/visible spectrophotometer	2×10^3–5×10^4	1
[a]Dose range depends on concentration of BLMG dye.			

Table S4. Comparison of the developed γ–dosimeter with previously reported γ–dosimeters based on organic dyes.

Dosimeter	Response mechanism (Analytical Method)	Detection Range (kGy)	Ref.
BLMG (20 μM)[a]	Chemical Reaction (Fluorescence)	6.0×10^{-6}–0.011	Our Method
Acid Fuchsin	Bleaching (UV-Vis)	0.17–1.65	2
Murexide dye	Degradation (UV-Vis)	0.1–2.0	3
DPC/Cr complex	Bleaching (UV-Vis)	0.2–1.0	4
Cyanocobalamin	Bleaching (UV-Vis)	0.2–1.0	5
Crystal violet	Bleaching (UV-Vis)	0.05–0.55	6
Rose bengal dye	Bleaching (UV-Vis)	0.05–1	7
4,4'-Di(1*H*-phenanthro[9,10-*d*]imidazole-2-yl)-biphenyl	Aggregation-induced quenching (Fluorescence)	7.0×10^{-6}–0.002	8
Tetraphenylethylene derivative	Aggregation-induced emission (Fluorescence)	2.3×10^{-5} – 0.008	9
Silole and polymer derivatives	Aggregation-induced emission (Fluorescence)	0.13–40	10
N-N'-bis(salicylidene)-1,3-propanediamine	Degradation (Fluorescence)	0.04–5	11
Thiamine Hydrochloride	Degradation (HPLC)	0.1–2.0	12
Benzene	Formation of phenol (HPLC)	7×10^{-6} – 0.1	13
Imino-BODIPY	Chemical Reaction (Fluorescence)	1.0×10^{-6}–0.005	14
[a]Dose range depends on concentration of BLMG dye.			

Table S5. Weight loss of chloroform solution of BLMG dye (80 μM) at 25 °C and 4 °C.

Sr No.	At 25 °C			At 4 °C		
	Initial Weight (Day 1) (g)	Final Weight (Day 20) (g)	Weight Loss (g)	Initial Weight (Day 1) (g)	Final Weight (Day 20) (g)	Weight Loss (g)
1	11.0258	11.0234	0.0024	11.0648	11.0642	0.0006
2	11.1305	11.1304	0.0001	11.2186	11.2185	0.0001
3	11.3527	11.3494	0.0033	11.3407	11.3399	0.0008
4	11.2983	11.2980	0.0003	11.3357	11.3354	0.0003
5	11.2767	11.2720	0.0047	11.5137	11.5137	0.0000

References

1. Dosimetry for Food Irradiation, Technical Reports Series No. 409, IAEA, Vienna, 2002.
2. M. Sayed, S. Tabassum, N. S. Shah, J. A. Khan, L. A. Shah, F. Rehman, S. U. Khan, H. M. Khan, M. Ullah, *J. Food Meas. Charact.* **2019**, *13*, 707–715.
3. S. M. Gafar, Abdel-Kader, N. M. *Pigment Resin Technol.* **2019**, *48*, 540–546.
4. S. M. Gafar, M. A. El-Kelany, S. R. El-Shawadfy, *J. Radiat. Res. Appl. Sci.* **2018**, *11*, 190–194.
5. V. Prakasan, B. Sanyal, S. P. Chawla, R. Chander, A. Sharma, *Appl. Radiat. Isot.* **2014**, *86*, 97–101.
6. H. M. Khan, S. Naz, S. Tabassum, *J. Radioanal. Nucl. Chem.* **2011**, *289*, 225–229.
7. H. M. Khan, A. A. Khan, *J. Radioanal. Nucl. Chem.* **2010**, *284*, 37–42.
8. J.-M. Han, M. Xu, B. Wang, N. Wu, X. Yang, H. Yang, B. J. Salter, L. Zang, *J. Am. Chem. Soc.* **2014**, *136*, 5090-5096.
9. X. Dong, F. Hu, Z. Liu, G. Zhang, D. Zhang, *Chem. Commun*. **2015**, *51*, 3892–3895.
10. Z. Liu, W. Xue, Z. Cai, G. Zhang, D. Zhang, *J. Mater. Chem.* **2011**, *21*, 14487-14491.
11. E. Ergun, *J. Fluoresc.* **2021**, *31*, 941–950.
12. Y. Li, C. Lv, Y. Zhao, Q. Sun, Y. Li, *Anal. Sci.* **2013**, *29*, 1189–1194.

13. K. Takeda, *Anal. Sci.* **2011**, *27*, 1189–1194.
14. Choudhary, M. K.; Gorai, S.; Patro, B. S. and Mula, S. *ChemPhotoChem*, **2024**, *8*, e202300245.